International Journal of Mechanical, Industrial and Aerospace Sciences
ISSN: 2517-9950
Vol:7, No:9, 2013

CFD Parametric Study of Mixers Performance

Mikhail Strongin

***Abstract*—**The mixing of two or more liquids is very common in many industrial applications from automotive to food processing. CFD simulations of these processes require comparison with test results. In many cases it is practically impossible. Therefore, comparison provides with scalable tests. So, parameterization of the problem is sufficient to capture the performance of the mixer.

However, the influence of geometrical and thermo-physical parameters on the mixing is not well understood.

In this work influence of geometrical and thermal parameters was studied. It was shown that for full developed turbulent flows (Re > $10^{4)}$, $Pe_t \approx$const and concentration of secondary fluid ~ F(**r**/*l*).

In other words, the mixing is practically independent of total flow rate and scale for a given geometry and ratio of flow rates of mixing flows. This statement was proved in present work for different geometries and mixtures such as EGR and water-urea mixture.

Present study has been shown that the best way to improve the mixing is to establish geometry with the lowest Pe_t number possible by intensifying the turbulence in the domain. This is achievable by using step geometry, impinging flow EGR on a wall, or EGR jets, with a strong change in the flow direction, or using swirler like flow in the domain or combination all of these factors. All of these results are applicable to any mixtures of no compressible fluids.

***Keywords*—**CFD, mixing, fluids, parameterization, scalability.

NOMENCLATURE

c_{Act} Concentration of secondary fluid
c_{id} Ratio of secondary fluid flow rate to total flow rate
D Pipe Diameter
D_{ric} Ricardo Device Diameter
h Clearance between Ricardo device and pipe wall
H Distance from Ricardo device centerline and beginning of elbow
k Turbulent kinetic energy
L1 Distance between sections A-A and B-B
L2 Distance from Ricardo device centerline and section B-B
L3 Length of elbow along centerline
L4 Distance from end of elbow and pipe
L5 Distance between section C-C and D-D
L6 Distance from section D-D to pipe outlet
M_{tot} Total Flow Rate
P_{air} Pressure at Air Inlet
P_{EG} Pressure at EGR Inlet
R1 Inner Radius of Elbow
R2 Outer Radius of Elbow
T_{air} Air Temperature
T_{EG} EGR Temperature
α Angle of Ricardo Device
ε Turbulent dissipation rate

Mikhail Strongin is with the Xylem Inc. AWS (e-mail: mikhail.strongin@xyleminc.com).

I. DESCRIPTION OF ANALYSIS

THEREFORE, many efforts are made to understand the mechanisms and principals of mixing processes. One of the main efforts is CFD modeling [1]–[5].

The mixing process in the EGR mixer and in pipe mixing of two liquids was simulated using CFD. Several different geometries are analyzed for EGR mixer and one for pipe mixing.

ICEM CFD is used for meshing of the model. Two types of mesh are prepared. First one is a tetra only mesh. The second one is a hybrid mesh combining a tetra mesh for one part of the domain and hexa mesh for another one. For the tetra only mesh, it takes more cells to obtain the same resolution as the hybrid mesh and is more expensive for calculations.

On the other hand, a hybrid mesh requires a coupling procedure, which, in these cases, causes some difficulties in convergence.

Steady state CFD calculations are performed with the assumption of incompressible flow and adiabatic wall, inlets, outlet boundary conditions. The density, specific heat, molecular viscosity, thermo conductivity, and diffusivity are assuming the same for EGR and air.

The realizable k – ε model was used for modeling of turbulence, because the realizable model is more sensitive to the effects of rapid streamline curvature than the standard k - ε model.

Figs. 1–5 show geometries for CFD analysis, parameters definition, boundary conditions, and the cases for CFD simulation are presented give in Tables I-IV.

TABLE I
SIMULATION CASES – EGR MIXER

Case	Dric (mm)	h (mm)	H (mm)	L1 (mm)	L2 (mm)	L3 (mm)	L4 (mm)	L5 (mm)	L6 (mm)	a (deg)	M_{tot} (kg/s)	C_{id}	T_{EGR} (°K)
3	43	10	N/A	250	250	102	33	N/A	N/A	180	0.4	15	505
4	43	10	N/A	65	435	102	33	N/A	N/A	180	0.4	15	505
6	43	10	N/A	250	250	102	33	N/A	N/A	180	0.3	7	505
7	43	10	N/A	250	250	102	33	N/A	N/A	180	0.3	7	450
9	43	10	64	N/A	N/A	102	N/A	130	140	0	0.4	15	505
10	43	10	64	N/A	N/A	102	N/A	130	140	0	0.4	15	505
11	43	10	64	N/A	N/A	102	N/A	130	140	0	0.4	15	505
12	43	10	64	N/A	N/A	102	N/A	130	140	90	0.4	15	505
13	43	10	64	N/A	N/A	102	N/A	130	140	90	0.4	15	505
14	43	10	64	N/A	N/A	102	N/A	130	140	90	0.4	15	505
15	43	10	64	N/A	N/A	102	N/A	130	140	180	0.4	15	505
16	43	10	64	N/A	N/A	102	N/A	130	140	180	0.4	15	505
17	43	10	64	N/A	N/A	102	N/A	130	140	180	0.4	15	505
18	43	10	64	N/A	N/A	102	N/A	130	140	0	0.4	15	505
19	43	20	64	N/A	N/A	102	N/A	130	140	0	0.4	15	505
20	43	20	64	N/A	N/A	102	N/A	130	140	0	0.4	15	505
21	43	20	64	N/A	N/A	102	N/A	130	140	180	0.4	15	505
22	43	20	64	N/A	N/A	102	N/A	130	140	180	0.4	15	505
23	43	20	64	N/A	N/A	102	N/A	130	140	180	0.4	15	505
24	43	10	64	N/A	N/A	102	N/A	130	140	180	0.7	15	505
25*	29	7	43	N/A	N/A	68	N/A	87	93	180	0.4	15	505
26*	64	15	96	N/A	N/A	152	N/A	195	210	180	0.4	15	505
27	43	10	64	N/A	N/A	102	N/A	130	140	180	0.4	21	505
28	43	10	64	N/A	N/A	102	N/A	130	140	180	0.4	15	355
29	43	10	64	N/A	N/A	102	N/A	130	140	0	0.4	15	355
30	34	10	60	N/A	N/A	102	N/A	130	140	180	0.4	21	505
31	51	4	69	N/A	N/A	102	N/A	130	140	180	0.4	15	505
32	51	4	69	N/A	N/A	102	N/A	130	140	180	0.4	21	505
33	51	4	69	N/A	N/A	102	N/A	130	140	180	0.5	34	505
34	51	4	69	N/A	N/A	102	N/A	130	140	0	0.4	15	505
35	51	4	69	N/A	N/A	102	N/A	130	140	0	0.5	34	505
36	51	4	69	N/A	N/A	102	N/A	130	140	90	0.4	15	505
37	51	4	69	N/A	N/A	102	N/A	130	140	90	0.5	34	505
38	51	4	69	N/A	N/A	102	N/A	130	140	0	0.4	15	355
39	51	4	69	N/A	N/A	102	N/A	130	140	0	0.5	34	355

*For cases 25 and 26 all linear parameters scale by factor 3/2 and 1.5 respectively

II. SUMMARY OF RESULTS

The following quantities are calculated on sections A-A, B-B, C-C, D-D and the outlet:

$$\sigma_f = ((\int \rho u_n (c_{Act} - c_{id})^2 dA) / \int \rho u_n dA)^{1/2} \quad (1)$$

$$\sigma_{fN} = \sigma_f / c_{id} \quad (2)$$

where u_n is a normal component of velocity to the section surface, ρ is mixture density, c_{Act} is the local secondary fluid concentration, c_{id} is a ratio of secondary fluid flow rate to total flow rate.

$$\sigma_a = ((\int (c_{Act} - c_{av})^2 dA) / A)^{1/2} \quad (3)$$

where A is an area of section surface

$$c_{av} = (\int c_{Act} dA) / A \quad (4)$$

The reason for examining the long tube geometry is to investigate the influence of the bend of the pipe on the mixing process in comparison with the straight pipe. The results show a relatively weak dependence of σ_{fN} on EGR % and EGR temperature for long tube cases. These results are presented in Table II.

TABLE II
EGR – LONG PIPE

Case	section	$\sigma_f\%/\sigma_{fN}$	$\sigma\%$
3	outlet	3.41/0.22	3.49
4	BB	5.34/0.35	5.32
6	outlet	1.39/0.19	1.32
7	outlet	1.35/0.19	1.30

Cases 3 – 4 show effect of bend
Cases 3 and 6 show effect of EGR%
Cases 6 – 7 show effect of temperature

The effect of the EGR device angle can be seen from a comparison of cases in Table VI. Comparing cases 4 (without the bend) and 11, 14 ,17 it is easy to see that the bend significantly improve the mixing process for the angles 0 and 180°, but for angle 90° the bend slightly deteriorates the

mixing in comparison with the straight pipe. The same tendency may be seen for different diameter of EGR device with ratio h/D = 0.0433 (cases 33, 35, and 37).

TABLE III
EGR MIXER – SHORT PIPE
RESULTS REPORTED ON OUTLET, INFLUENCE OF PARAMETER α

Case	Angle α (°)	σ_f%/ σ_{fN}	σ_a%
11	0	4.21/ 0.28	4.31
14	90	6.16/0.41	5.96
17	180	3.78/0.25	3.6
35	0	5.9/0.17	5.56
37	90	7.84/0.23	7.95
33	180	6.93/0.20	6.8

Results in Table IV show the influence of the value of clearance height, h, on the mixing process. It can be seen here (cases 11 and 20 for $\alpha = 0^o$& cases 17 and 23 for $\alpha = 180^o$) that mixing for different h with different angles (0^o and 180^o) change in different directions

TABLE IV
EGR MIXER – SHORT PIPE
RESULTS REPORTED ON OUTLET INFLUENCE OF PARAMETER h

Case	h/D	σ_f%/σ_{fN}	σ_a%
11	0,0984	4.21/0.28	4.31
20	0.1968	3.93/0.26	4.22
17	0,0984	3.78/0.25	3.6
23	0.1968	5.89/0.39	5.61

The results shown in Table V indicate that for the EGR mixer domain with similar geometry (differing only by linear scale) and constant EGR %, the index of mixing σ_f is practically the same for linear scale changes up to 2.25 times.

TABLE V
RESULTS REPORTED ON OUTLET INFLUENCE OF LINEAR SCALING

Case	Scale	σ_f%/σ_{fN}	σ_a%
17	1	3.78/0.25	3.58
25	2/3	3.82/0.25	3.62
26	1.5	3.76/0.25	3.58

Table VI presents the results for the EGR mixer domain with similar geometry (differing only by total flow rate) and constant EGR %. The index of mixing $\sigma_f$is the same with a change in the flow rate up to 2 times.

The physical explanation of this phenomenon will be given in the discussion results.

It is important to say that, as shown in this observation, the total flow rate has no influence on the mixing process and it is possible to compare other parameters without considering the flow rate.

TABLE VI
RESULTS REPORTED ON OUTLET, INFLUENCE OF PARAMETER M_{TOT}

Case	M_{tot} (kg/s)	σ_f%/σ_{fN}	σ_a%
17	0.36	3.78/0.25	3.58
24	0.715	3.82/0.25	3.62

Table VII shows results with different EGR % than in previous cases. For different EGR % the normalized standard deviation of EGR concentration, $\sigma_{fN,}$ is a very convenient index for mixing estimation. Comparing the results from cases 17 and 27 with 15% and 21% EGR respectively, one may say that σ_{fN} or mixing is only slightly changed. Cases 17 and 27 have ratio D_{ric} / D = 0.42; for cases 32 and 33 - D_{ric} / D =0.504.

Comparing results from cases 40 and 41for new design mixer with 21% and 34.4% EGR respectively, one may say that σ_{fN} or mixing, in contrary to EGR mixing, is significantly changed.

The physical explanation of this phenomenon will be given in discussion of results.

TABLE VII
RESULTS REPORTED ON OUTLET INFLUENCE OF EGR%

Case	EGR%	σ_f%/ σ_{fN}	σ_a%
17	15.1	3.78/0.25	3.58
27	21	5.62/0.27	5.56
32	21.1	4.43/0.21	5.22
33	34.3	6.93/0.20	6.8

Table VIII shows results for cases with different temperatures. Cases 11 – 29 have a ratio D_{ric} / D = 0.42; for cases 34 – 39 D_{ric} / D =0.504. It should be emphasized that temperature changes influence the mixing index, σ_{fN}, for different angles (0^o and 180^o) of EGR device (cases11, 29 and 17, 28).

The physical explanation of this phenomenon will be given in discussion of results.

TABLE VIII
RESULTS REPORTED ON OUTLET INFLUENCE OF TEMPERATURE

Case	Temperature EGR	σ_f%/σ_{fN}	σ_a%
17	505	3.78/0.25	3.58
28	355	4.84/0.32	4.67
11	505	4.21/0.28	4.31
29	355	3.96/0.26	4
34	505	3.65/0.24	3.88
38	355	3.73/0.25	3.92
35	505	5.9/0.17	5.56
39	355	5.48/0.16	5.44

Table IX presents results with different ratio D_{ric} / D. The interesting result here is the significantly increasing σ_{fN}, or decreasing mixing, for case 30 (D_{ric} / D = 0.34) in comparison with case 27 where this ratio is 0.42

TABLE IX
EGR MIXER – SHORT PIPE
RESULTS REPORTED ON OUTLET INFLUENCE OF PARAMETER D_{RIC} / D

Case	σ_f%/σ_{fN}	σ_a%
30	12.2/0.58	12.7
27	5.62/0.27	5.56

Table X presents results on outlet for two pipes mixer of water-urea mixture.

TABLE X
2 PIPES MIXING σ_F AND σ_{FN} ON OUTLET (C_{ID} = 0.25)

M_{tot} (kg/s)	σ_f %	σ_{fN}
8	6.29	0.25
4	5.97	0.24
2	5.10	0.20

III. DISCUSSION OF RESULTS

The results shown in Tables VI and X have the following physical explanation.

The concentration distribution, C, obtained from the diffusion equation in this case, has to be a function of non-dimensional parameters **r**/*l* and, the turbulent Peclet number, $Pe_t = Ul/D_t$:

$$C \sim F(\mathbf{r}/l, Pe_t) \quad (5)$$

where **r** – is the position vector of the point in the domain in which the concentration is measured (computed), *l* is a linear scaling factor, U is the characteristic velocity, and D_t is the turbulent diffusion coefficient.

D_t is approximated as $D_t \sim k^2/\varepsilon$, where k and ε are taken from calculation of the k-ε turbulence model, and $k \sim U^2$, $\varepsilon \sim U^3/l$.

In this case $Pe_t \approx$const and the expression (1) can be rewritten as:

$$C \sim F(\mathbf{r}/l) \quad (6)$$

In other words, the mixing is practically independent of total flow rate and scale for a given geometry and secondary fluid %.

As can be seen in Table III, the bend significantly improves the mixing process for the angles 0 and 180°, but for angle 90°, the bend slightly deteriorates the mixing when compared with the straight tube. There is an explanation of this phenomenon: the recirculation zone responsible for better mixing in the elbow tube has practically no effect on the EGR stream in the case of 90°EGR devise location.

The temperature influence on the mixing process for EGR mixer with the long pipe is very weak (cases 6, 7), because in the elbow area, when temperature may be influence the mixing process, the temperature difference is relatively low.

For the short pipe, temperature and the clearance between EGR device and tube wall may have some influence on the mixing process.

Table III gives the dependence of mixing on the angle of location of EGR device. The worst case is, as expected, with the angle 90°. The explanation of this phenomenon is shown above.

The 180° location of EGR mixer gives a little bit better result in comparison with 0° location. The physical explanation of this effect will be given later with explanation of temperature effects.

Comparing the results from Table IV for different h, it is easy to see the results of mixing for different angles (0° and 180°) change in different directions. It seems that this effect has the same explanation as the previous one.

The influence of EGR temperature on the mixing process of EGR device is presented in Table VIII. It can be seen from Fig. 6, that the best result for mixing is the case where the cold gas is near the small radius of the elbow and hot gas is closer to large radius.

A centrifugal force acting on gas acting on the gas leads, in this case, to a more unstable situation and, as a consequence, to better mixing.

The results in Table IX show that the decreasing ratio D_{ric}/ D to 0.34 (case 30) from 0.42 (case 27) increases σ_{Fn} from 0.27 (case 27) to 0.58 (case 30). It permits one to make a conclusion that decreasing ratio D_{ric}/ D lower than 0.4 significantly deteriorates mixing parameters.

It may see from Table VII that the influence of EGR% on $\sigma_{Fn}$is not significant but visible for EGR mixer.

In most cases for the EGR mixer, increasing EGR% leads to decreasing σ_{fN} when other parameters are constant.

Apparently, this effect is caused by higher shear stress in the shear layer between air and EGR flows, which may increases D_t. The result of case 27 may be explained by the influence of two factors: first is a higher shear stress and second is significantly thinner cold flow layer near the inner radius wall of the elbow. Evidently, in this case, the second effect prevails.

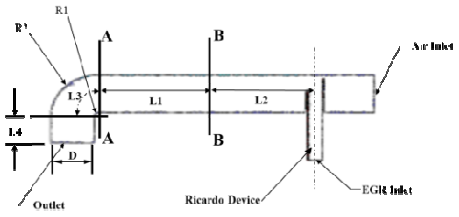

$L_r = L1 + L2 + L3 + L4$ (w/ elbow)

$L_r = L1 + L2$ (w/o elbow)

$L3 = \pi(R1+R2)/4$

Fig. 1 Schematic of EGR Geometry (Long Tube)

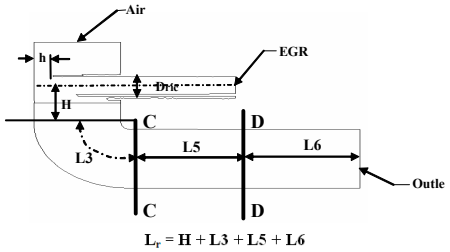

$L_r = H + L3 + L5 + L6$

Fig. 2 Schematic of EGR Geometry (Short Tube)

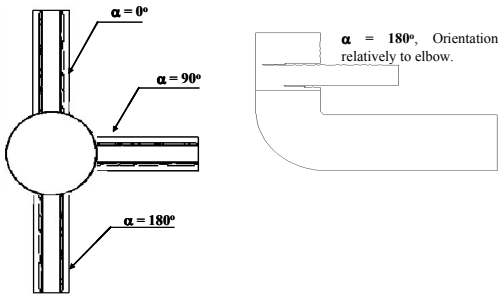

Fig. 3 Definition of EGR Angle

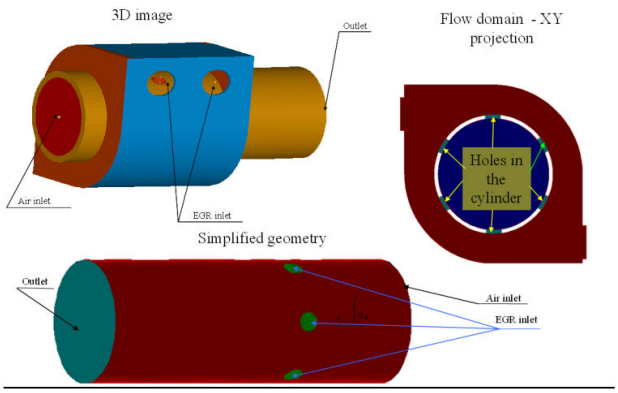

Fig. 4 EGR Mixer Geometries

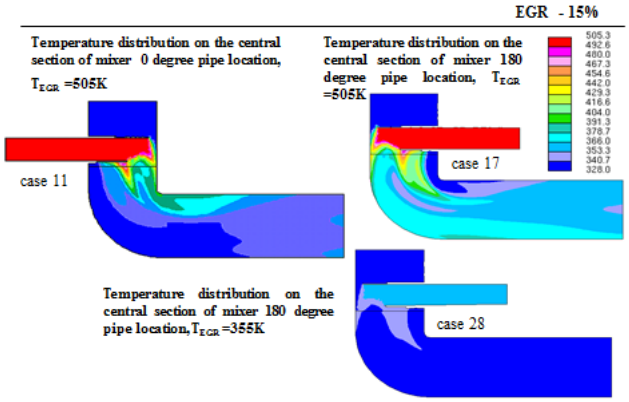

Fig. 5 EGR mixer – Temperature distribution on the central section

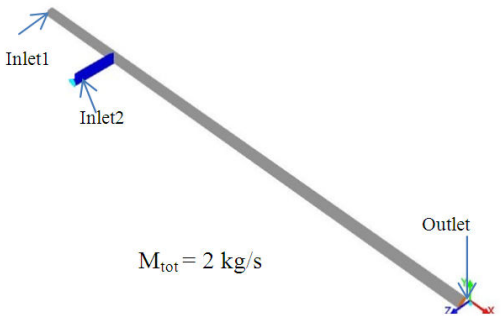

Fig. 6 Geometry of 2 pipes mixer

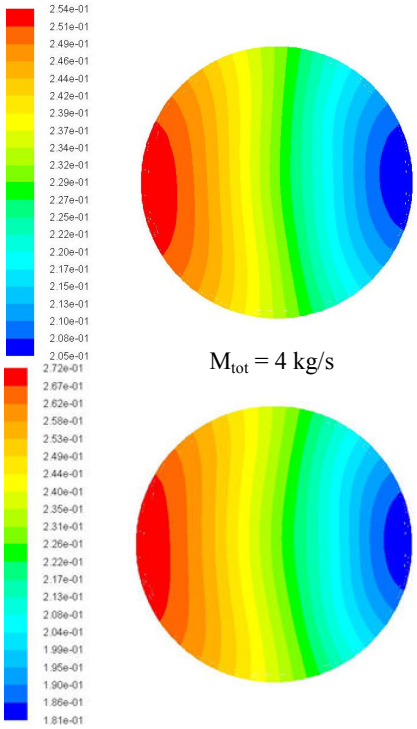

Fig. 7 C_{Act} on 2 pipes mixer outlet

IV. Conclusions

For EGR mixer with a bend the angle for Ricardo device location should be 0^{o} or 180^{o}.

For the EGR mixer the ratio D_{ric} / D should be 0.4 – 0.5.

This is achievable by using step geometry, impinging flow EGR on a wall, or EGR jets, with a strong change in the flow direction, or using swirler like flow in the domain or combination all of these factors.

The best way to improve the mixing is to establish geometry with the lowest Pe_t number possible by intensifying the turbulence in the domain.

References

[1] A.K. Sahu, P. Kumar, A.W. Patwardhan, J.B. Joshi, (1999)CFD modelling and mixing in stirred tanks, Chemical Engineering Science, Volume 54, Issues 1314, July 1999, Pages 2285–2293

[2] C. G. Giannopapa B. J., van der Linden, W. van Druten, M. Bongers (2008), Modeling the mixing process of liquids with concentrates in capsules,2008 ASME Pressure Vessels and Piping Division Conference, PVP 2008-6133.

[3] 2. Mikhail P. Strongin, Vadim Strots (2007). CFD Simulation of Urea Evaporation and Mixing. 1st Conference: MinNOx – Minimization of NOx Emissions Through Exhaust Aftertreatment, February 1-2,Berlin, Germany.

[4] Kevin Breisacher and Jeffrey Moder (2010), Computational Fluid Dynamics (CFD) Simulations of Jet Mixing in Tanks of Different Scales, NASA/TM—2010-216749, p.1-26.

[5] Mikhail P. Strongin, CFD Modeling of Mixing Process in Pump for Two Liquids with Different Temperatures, Proceedings of FEDSM2009,FEDSM-ICNMM2010-30969